LETTER

doi:10.1038/nature11933

Carbon monoxide in clouds at low metallicity in the dwarf irregular galaxy WLM

Bruce G. Elmegreen[1], Monica Rubio[2], Deidre A. Hunter[3], Celia Verdugo[2], Elias Brinks[4] & Andreas Schruba[5]

Carbon monoxide (CO) is the primary tracer for interstellar clouds where stars form, but it has never been detected in galaxies in which the oxygen abundance relative to hydrogen is less than 20 per cent of that of the Sun, even though such 'low-metallicity' galaxies often form stars. This raises the question of whether stars can form in dense gas without molecules, cooling to the required near-zero temperatures by atomic transitions and dust radiation rather than by molecular line emission[1]; and it highlights uncertainties about star formation in the early Universe, when the metallicity was generally low. Here we report the detection of CO in two regions of a local dwarf irregular galaxy, WLM, where the metallicity is 13 per cent of the solar value[2,3]. We use new submillimetre observations and archival far-infrared observations to estimate the cloud masses, which are both slightly greater than 100,000 solar masses. The clouds have produced stars at a rate per molecule equal to 10 per cent of that in the local Orion nebula cloud. The CO fraction of the molecular gas is also low, about 3 per cent of the Milky Way value. These results suggest that in small galaxies both star-forming cores and CO molecules become increasingly rare in molecular hydrogen clouds as the metallicity decreases.

Wolf–Lundmark–Melotte (WLM) is an isolated dwarf galaxy at the edge of the Local Group[4]. It has a low star-formation rate because of its small size and, like other dwarf irregular (dIrr) galaxies, shows no previous evidence[5] for the molecular gas that always accompanies young stars in larger galaxies[6]. One problem with the detection of molecules is that the dominant tracer of such gas is CO, and dIrr galaxies have low carbon and oxygen abundances relative to hydrogen. No galaxy with an O/H abundance less than 20% has been detected using CO as a tracer[7–9]. Far more abundant is molecular hydrogen (H_2), but this does not have an observable state of excitation at the low temperatures (~10–30 K) required for star formation.

To search for star-forming gas, we surveyed WLM for CO($J = 3$–2) emission in rotational state J and for continuum dust emission at 345 GHz using the Atacama Pathfinder Experiment (APEX) telescope at Llano de Chajnantor, Chile, with the Swedish Heterodyne Facility Instrument[10] and the Large APEX Bolometer Camera[11] (LABOCA). We also used a map of dust emission at 160 μm from the Spitzer Local Volume Legacy Survey[12] and a map of atomic hydrogen re-reduced from the archives of the Jansky Very Large Array radio telescope. The dust measurements can be converted to a dust temperature and a dust mass, and, after applying a suitable gas-to-dust ratio, to a gas mass from which the H I mass can be subtracted to give the H_2 mass for comparison with CO.

Figure 1 shows WLM and the two regions, designated A and B, where we detected CO(3–2) emission, along with H I, far-infrared (FIR) and submillimetre images. Observed and derived parameters are listed in Tables 1 and 2, respectively. The peak CO brightness temperature in each detected region is ~0.01–0.015 K and the line-width is ~12 km s^{-1} (full-width at half-maximum). Previous efforts to detect CO($J = 1$–0) in WLM[5] partly overlapped region A with a 45″ aperture and determined a 5σ upper limit to the CO(1–0) intensity of 0.18 K km s^{-1}. Our observation with an 18″ aperture yields an intensity of 0.200 ± 0.046 K km s^{-1} for CO(3–2) in the same region. The difference arises because the CO cloud is unresolved even by our 18″ beam—we did not detect comparable CO(3–2) intensities in our searches adjacent to region A. The previous upper limit corresponds to a maximum CO(1–0) luminosity of 8,300 K km s^{-1} pc^2 inside 45″ (which corresponds to a beam diameter of 215 pc at WLM), whereas the cloud we detect has a CO(3–2) luminosity ~6 times smaller (1,500 K km s^{-1} pc^2). Likewise, the previous null detection[5] in CO($J = 2$–1) claimed a 5σ upper limit that is about the same as our CO(3–2) detection, but their closest pointing differed from region A by ~70 pc (14″, or half the beam diameter for CO(2–1)), which could have been enough to take it off the CO cloud.

The 160-μm, 870-μm and H I peaks are slightly offset from the CO positions, indicating variations in temperature and molecular fraction. A large H I and FIR cloud that surrounds region A, designated region A1, was used to measure the dust temperature, $T_d \sim 15$ K, which was assumed to be the same throughout the region (the 160-μm observation does not resolve region A, and so a more localized temperature measurement is not possible). We determined T_d from the 870-μm and 160-μm fluxes corrected for the CO(3–2) line and broadband free–free emission (Table 1), assuming a modified black-body function with dust emissivity proportional to frequency to the power β. Local measurements[13] suggest that $\beta = 1.78 \pm 0.08$, although a range is possible[14,15], depending on grain temperature and properties[16]. The 870-μm flux was also corrected for an unexplained FIR and submillimetre excess that is commonly observed in other low-metallicity galaxies[17,18]. An alternate

Table 1 | Observations of WLM

Source	Region	Right ascension	Declination	Beam diameter (″)	Flux
CO(3–2)	A	0 h 1 min 57.32 s	−15° 26′ 49.5″	18	0.200 ± 0.046 K km s^{-1}
H I	A	0 h 1 min 57.32 s	−15° 26′ 49.5″	22	774 ± 40 mJy km s^{-1}
870 μm	A	0 h 1 min 57.32 s	−15° 26′ 49.5″	22	2.66 ± 0.53 mJy (0.11, 0.02)*
H I	A1	0 h 1 min 56.93 s	−15° 26′ 40.84″	45	4,170 ± 82 mJy km s^{-1}
870 μm	A1	0 h 1 min 56.93 s	−15° 26′ 40.84″	45	15.2 ± 3.0 mJy (0.11, 0.06)*
160 μm	A1	0 h 1 min 56.93 s	−15° 26′ 40.84″	45	136.2 ± 13.6 mJy (0.05)†
CO(3–2)	B	0 h 2 min 1.68 s	−15° 27′ 52.5″	18	0.129 ± 0.032 K km s^{-1}

* Quantities in parentheses are the CO(3–2) flux and the free–free emission, both in mJy, that were subtracted from the source flux before calculating the dust flux.
† Quantity in parentheses is the free–free emission, in mJy, that was subtracted from the source flux before calculating the dust flux. The average FIR excess factor[18] for the Small Magellanic Cloud (SMC) is 1.7, so we divide the CO-corrected and free–free-corrected 870-μm fluxes in the table by 1.7 to get the thermal dust flux.

[1]IBM Research Division, T.J. Watson Research Center, 1101 Kitchawan Road, Yorktown Heights, New York 10598, USA. [2]Departamento de Astronomía, Universidad de Chile, Casilla 36-D, Santiago, Chile. [3]Lowell Observatory, 1400 West Mars Hill Road, Flagstaff, Arizona 86001, USA. [4]Centre for Astrophysics Research, University of Hertfordshire, Hatfield AL10 9AB, UK. [5]Cahill Center for Astronomy and Astrophysics, California Institute of Technology, Pasadena, California 91125, USA.

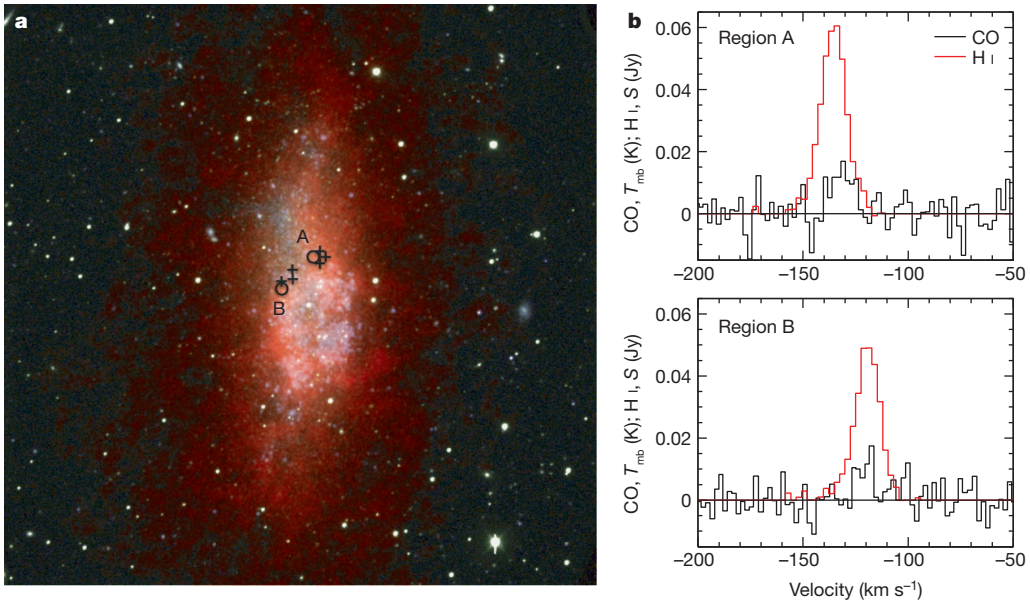

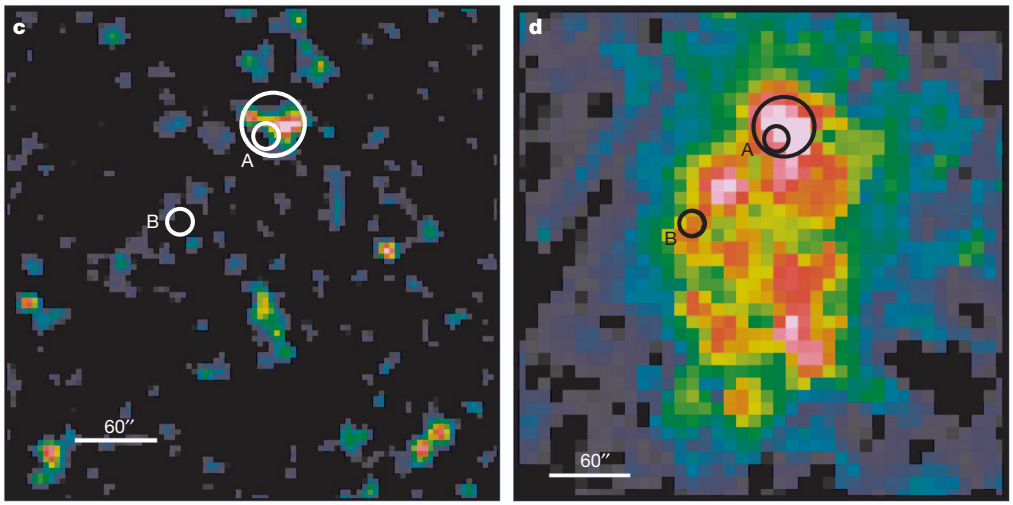

Figure 1 | Observations of the galaxy WLM. WLM is a small, gas-rich galaxy 985 ± 33 kpc from the Milky Way[4]. It contains $1.6 \times 10^7 M_\odot$ of stars[28], compared with $(6.4 \pm 0.6) \times 10^{10} M_\odot$ in the Milky Way[29], and it forms new stars at a rate[23] of $0.006 M_\odot$ yr^{-1}, which is 12 times higher per unit stellar mass than the Milky Way[30]. **a**, Colour composite image: red, H I; green, V band; blue, GALEX far-ultraviolet. For H I the aperture was 7.6′′ and the resolution was 2.6 km s^{-1}, and for CO(3–2) the aperture was 18′′ (circles) and the resolution was 0.11 km s^{-1}, although the CO(3–2) spectra shown in the figure were smoothed to a resolution of 2.2 km s^{-1}. The CO detections are labelled; their exposure times were 218 min (region A) and 248 min (region B). Other regions searched with exposure times shorter by factors of ~2 to ~6 are indicated by plus signs; the presence of comparable CO mass in some of these other regions cannot be ruled out. **b**, Spectra of the two detections: velocities are relative to the local standard of rest; CO labels main-beam brightness temperature, T_{mb}, in kelvin; H I labels flux in Jy. **c**, False-colour image of the 870-μm observations made with LABOCA on APEX. **d**, False-colour Spitzer 160-μm image obtained from Spitzer archives. In **c** and **d**, the images show the same field of view and the small circles (22′′ diameter, the resolution of LABOCA) show where CO was detected. The large circle is 45′′ in diameter and surrounds a large H I and FIR cloud (region A1) where the dust temperature was measured.

Table 2 | Derived quantities for WLM

Source	Region	T (K)	Σ^* ($M_\odot$ pc^{-2})	Mass ($M_\odot$)
$\beta = 1.8$, $\alpha_{CO} = 124 \pm 60$†				
Dust	A	14.7 ± 0.7‡	0.053 ± 0.014	$(4.6 \pm 1.2) \times 10^2$
Gas§	A		$(58 \pm 15)\delta_{GD}$	$((5.1 \pm 1.3) \times 10^5)\delta_{GD}$
H II	A		27.3 ± 1.4	$(2.4 \pm 0.1) \times 10^5$
H_2	A		31 ± 15	$(1.8 \pm 0.8) \times 10^5$
H_2¶	B		20 ± 10	$(1.2 \pm 0.6) \times 10^5$
$\beta = 1.6$, $\alpha_{CO} = 34 \pm 34$†				
Dust	A	15.9 ± 0.8‡	0.032 ± 0.008	$(2.8 \pm 0.7) \times 10^2$
Gas§	A		$(36 \pm 9)\delta_{GD}$	$((3.1 \pm 0.8) \times 10^5)\delta_{GD}$
H_2	A		8.3 ± 9	$(0.5 \pm 0.5) \times 10^5$
H_2¶	B		5.3 ± 6	$(0.3 \pm 0.3) \times 10^5$
$\beta = 2$, $\alpha_{CO} = 271 \pm 97$†				
Dust	A	13.6 ± 0.6‡	0.087 ± 0.022	$(7.5 \pm 1.9) \times 10^2$
Gas§	A		$(95 \pm 24)\delta_{GD}$	$((8.3 \pm 2.1) \times 10^5)\delta_{GD}$
H_2	A		67 ± 24	$(3.9 \pm 1.4) \times 10^5$
H_2¶	B		44 ± 16	$(2.5 \pm 0.9) \times 10^5$

* Mass column density of gas or dust.
† The units of α_{CO} are $M_\odot$ pc^{-2} K^{-1} km^{-1} s. The uncertainty is dominated by the uncertainties in the 160-μm and 870-μm fluxes, as indicated by their error limits in Table 1. The error limits are approximately symmetric.
‡ The dust temperature in region A is assumed to be the same as the measured dust temperature in region A1.
§ $\delta_{GD} = R_{GD}/1{,}100$ is the gas-to-dust ratio, R_{GD}, normalized by the solar value and scaled to the metallicity of WLM. Lowering δ_{GD} lowers α_{CO}, but this does not seem reasonable: data suggests that the gas-to-dust mass ratio is ~5,000 for 12 + log(O/H) = 7.8 (ref. 27), and this implies larger values of δ_{GD} (~4.5) and α_{CO}. The gas mass and resulting α_{CO} value also depend on the assumed correction factor of 1.7 for submillimetre excess. With no correction for this excess, α_{CO} increases for all β values: at $\beta = 1.8$, $\alpha_{CO} = 370$. Solutions with no submillimetre excess correction and lower β values[19] can be found in Supplementary Information. In addition, α_{CO} depends on the assumed value of CO(3–2)/CO(1–0), which was taken to be 0.8 in Table 2; a value of CO(3–2)/CO(1–0) = 1 increases α_{CO} to 155 for $\beta = 1.8$.
|| The H I mass column density is corrected for helium and heavy elements.
¶ The molecular mass for region B was calculated using the CO integrated intensity and the value of α_{CO} determined from region A.

combination of lower β with no submillimetre correction[19] gives similar results (Supplementary Information). The dust mass was calculated from an emissivity[14] of $\kappa = 13.9\,\mathrm{cm^2\,gm^{-1}}$ at 140 μm, and converted to 870 μm with the same power-law index, β. The dust mass for region A is then $M_{\mathrm{dust,A}} = S_{870,\mathrm{A}}D^2/\kappa B_\nu(T_\mathrm{d})$ for flux $S_{870,\mathrm{A}}$, distance D and black-body spectral function B_ν.

Dust mass is converted to gas mass using a factor equal to the gas-to-dust mass ratio, R_{GD}. An approximation[8] is to assume the solar value[20] (1/0.007) increased by the inverse of the metallicity of WLM (0.13), which would give 1,100. We use this approximation here, but introduce a scaling factor to the gas mass, $\delta_{\mathrm{GD}} = R_{\mathrm{GD}}/1{,}100$; that is, the gas-to-dust ratio normalized by the solar value and scaled to the metallicity.

The results are in Table 2, assuming $\beta = 1.8$ as the fiducial value and comparing the results with those for $\beta = 1.6$ and 2 to illustrate the dependence of the results on β. Dust and gas mass correlate[15] with the assumed β value. The total gas mass column density in a 22″ region around region A is $\sim 58 \pm 15 M_\odot\,\mathrm{pc^{-2}}$ for $\beta = 1.8$ ($M_\odot$, solar mass). Atomic hydrogen contributes $\sim 27.3 \pm 1.4 M_\odot\,\mathrm{pc^{-2}}$, and the remainder is ascribed to molecular H_2 traced by the observed CO.

The integral under the CO(3–2) line from region A is $I_{\mathrm{CO}} = 0.200 \pm 0.046\,\mathrm{K\,km\,s^{-1}}$. This intensity has to be converted to CO(1–0) before comparing it with H_2 mass in the conventional way. We take as a guide[21] the value of CO(3–2)/CO(1–0) ≈ 0.80 in another low-metallicity galaxy, the SMC[22] (where O/H = 20% of the solar value). The result, $0.25\,\mathrm{K\,km\,s^{-1}}$, is combined with the H_2 mass column density to determine the conversion factor, α_{CO}, from CO(1–0) to H_2. If α_{CO} can be calibrated as a function of metallicity, then CO observations can be used directly to infer the molecular gas content irrespective of the dust spectral energy distribution. Extensive compilations[7–9] show α_{CO} increasing strongly at lower metallicity, from $\sim 4 M_\odot\,\mathrm{pc^{-2}\,K^{-1}\,km^{-1}\,s}$ in the Milky Way[8], where the metallicity[3] is 12 + log(O/H) = 8.69, down to the previous CO detection limit[8] in the SMC, where $\alpha_{\mathrm{CO}} \approx 70 M_\odot\,\mathrm{pc^{-2}\,K^{-1}\,km^{-1}\,s}$ at 12 + log(O/H) = 8.0. Our observations of WLM[2] at a metallicity of 12 + log(O/H) = 7.8 continue this trend.

Taking the H_2 column density from the residual between the dust-derived total and the H I column density, $31 \pm 15 M_\odot\,\mathrm{pc^{-2}}$, and dividing by the inferred CO(1–0) line integral of $0.25\,\mathrm{K\,km\,s^{-1}}$, we obtain $\alpha_{\mathrm{CO}} = 124 \pm 60 M_\odot\,\mathrm{pc^{-2}\,K^{-1}\,km^{-1}\,s}$ including helium and heavy elements, with a range in α_{CO} from 34 to 271 as β varies from 1.6 to 2. The corresponding factor, X_{CO}, for conversion from I_{CO} to H_2 column density would be $(5.8 \pm 2.8) \times 10^{21}\,\mathrm{cm^{-2}\,K^{-1}\,km^{-1}\,s}$, ranging from 1.5×10^{21} to 1.3×10^{22} as β varies between 1.6 and 2. There is a large uncertainty because of the unknown dust properties (β, κ, δ_{GD} and the submillimetre excess) and molecular excitation (CO(3–2)/CO(1–0)) in dIrr galaxies.

The star-formation rate based on the Hα and far-ultraviolet[23] fluxes within an 18″ aperture centred on cloud A is $(3.9\text{–}4.8) \times 10^{-5} M_\odot\,\mathrm{yr^{-1}}$. Dividing these rates into the CO-associated molecular mass using $\alpha_{\mathrm{CO}} = 124\,M_\odot\,\mathrm{pc^{-2}\,K^{-1}\,km^{-1}\,s}$ gives a CO molecular consumption time (for converting gas into stars) of 4.6–3.8 Gyr for region A. In region B, the star-formation rate from Hα and far-ultraviolet fluxes is $(1.7\text{–}12.6) \times 10^{-5} M_\odot\,\mathrm{yr^{-1}}$ and the CO molecular consumption time is 6.7–1.5 Gyr. These times are only slightly larger than the average value in spiral galaxies[24], which is ~2 Gyr, but they are ten times larger than the rate per molecule in local giant molecular clouds[25], which is a more direct analogy with our observations.

The detection of CO in WLM suggests that star formation continues to occur in dense molecular gas even at lower metallicities than previously observed. The similarity between the metallicities of dIrr galaxies such as WLM and those of larger galaxies at high redshift[26] implies that we should be able to study star formation in young galaxies using the usual techniques.

Received 24 October 2012; accepted 23 January 2013.

1. Krumholz, M. R. Star formation in atomic gas. *Astrophys. J.* **759,** 9 (2012).
2. Lee, H., Skillman, E. D. & Venn, K. A. Investigating the possible anomaly between nebular and stellar oxygen abundances in the dwarf irregular galaxy WLM. *Astrophys. J.* **620,** 223–237 (2005).
3. Asplund, M., Grevesse, N., Sauval, A. J. & Scott, P. The chemical composition of the sun. *Annu. Rev. Astron. Astrophys.* **47,** 481–522 (2009).
4. Leaman, R. *et al.* The resolved structure and dynamics of an isolated dwarf galaxy: a VLT and Keck spectroscopic survey of WLM. *Astrophys. J.* **750,** 33 (2012).
5. Taylor, C. L. & Klein, U. A search for CO in the Local Group dwarf irregular galaxy WLM. *Astron. Astrophys.* **366,** 811–816 (2001).
6. Bigiel, F. *et al.* A constant molecular gas depletion time in nearby disk galaxies. *Astrophys. J.* **730,** L13 (2011).
7. Taylor, C. L., Kobulnicky, H. A. & Skillman, E. D. CO emission in low-luminosity, H I-rich galaxies. *Astron. J.* **116,** 2746–2756 (1998).
8. Leroy, A. K. *et al.* The CO-to-H_2 conversion factor from infrared dust emission across the Local Group. *Astrophys. J.* **737,** 12 (2011).
9. Schruba, A. *et al.* Low CO luminosities in dwarf galaxies. *Astron. J.* **143,** 138 (2012).
10. Vassilev, V. *et al.* A Swedish heterodyne facility instrument for the APEX telescope. *Astron. Astrophys.* **490,** 1157–1163 (2008).
11. Siringo, G. *et al.* The Large APEX BOlometer CAmera LABOCA. *Astron. Astrophys.* **497,** 945–962 (2009).
12. Dale, D. A. *et al.* The Spitzer Local Volume Legacy: survey description and infrared photometry. *Astrophys. J.* **703,** 517–556 (2009).
13. Planck Collaboration *et al.* Planck early results. XXV. Thermal dust in nearby molecular clouds. *Astron. Astrophys.* **536,** A25 (2011).
14. Draine, B. T. Interstellar dust grains. *Annu. Rev. Astron. Astrophys.* **41,** 241–289 (2003).
15. Galametz, M. *et al.* Mapping the cold dust temperatures and masses of nearby KINGFISH galaxies with Herschel. *Mon. Not. R. Astron. Soc.* **425,** 763–787 (2012).
16. Coupeaud, *et al.* Low-temperature FIR and submillimetre mass absorption coefficient of interstellar silicate dust analogues. *Astron. Astrophys.* **535,** A124 (2011).
17. Galametz, M. *et al.* Probing the dust properties of galaxies up to submillimetre wavelengths. II. Dust-to-gas mass ratio trends with metallicity and the submm excess in dwarf galaxies. *Astron. Astrophys.* **532,** A56 (2011).
18. Verdugo, C. *Sub-Millimeter Studies of Cold Dust and Gas in the Magellanic Clouds.* MSc thesis, Univ. Chile (2012).
19. Planck Collaboration. *Planck* early results. XVII. Origin of the submillimetre excess dust emission in the Magellanic Clouds. *Astron. Astrophys.* **536,** A17 (2011).
20. Draine, B. T. *et al.* Dust masses, PAH abundances, and starlight intensities in the SINGS galaxy sample. *Astrophys. J.* **663,** 866–894 (2007).
21. Nikolić, S., Garay, G., Rubio, M. & Johansson, L. E. B. CO and CS in the Magellanic Clouds: a χ^2-analysis of multitransitional data based on the MEP radiative transfer model. *Astron. Astrophys.* **471,** 561–571 (2007).
22. Dufour, R. J. The composition of H II regions in the Magellanic Clouds. *IAU Symp.* **108,** 353–360 (1984).
23. Hunter, D. A., Elmegreen, B. G. & Ludka, B. C. *GALEX* ultraviolet imaging of dwarf galaxies and star formation rates. *Astron. J.* **139,** 447–475 (2010).
24. Leroy, A. K. *et al.* The star formation efficiency in nearby galaxies: measuring where gas forms stars effectively. *Astron. J.* **136,** 2782–2845 (2008).
25. Lada, C. J., Forbrich, J., Lombardi, M. & Alves, J. F. Star formation rates in molecular clouds and the nature of the extragalactic scaling relations. *Astrophys. J.* **745,** 190 (2012).
26. Mannucci, F. *et al.* LSD: Lyman-break galaxies, stellar populations and dynamics – I. Mass, metallicity and gas at $z \sim 3.1$. *Mon. Not. R. Astron. Soc.* **398,** 1915–1931 (2009).
27. Engelbracht, C. W. *et al.* Metallicity effects on dust properties in starbursting galaxies. *Astrophys. J.* **678,** 804–827 (2008).
28. Zhang, H.-X., Hunter, D. A., Elmegreen, B. G., Gao, Y. & Schruba, A. Outside-in shrinking of the star-forming disks of dwarf irregular galaxies. *Astron. J.* **143,** 47 (2012).
29. McMillan, P. J. Mass models of the Milky Way. *Mon. Not. R. Astron. Soc.* **414,** 2446–2457 (2011).
30. Chomiuk, L. & Povich, M. S. Toward a unification of star formation rate determinations in the Milky Way and other galaxies. *Astron. J.* **142,** 197 (2011).

Supplementary Information is available in the online version of the paper.

Acknowledgements This work was funded in part by the US National Science Foundation through grants AST-0707563 and AST-0707426 to D.A.H. and B.G.E. M.R. and C.V. wish to acknowledge support from CONICYT (FONDECYT grant no. 1080335). M.R. was also supported by the Chilean Center for Astrophysics FONDAP grant no. 15010003. A.S. was supported by the Deutsche Forschungsgemeinschaft Priority Program 1177. We are grateful to M. Albrecht for help with the LABOCA data reduction and to L. Hill for making Fig. 1a. The National Radio Astronomy Observatory is a facility of the US National Science Foundation operated under cooperative agreement by Associated Universities, Inc.

Author Contributions B.G.E. coordinated the observational team, did the calculations for Table 2 and wrote the manuscript; M.R. was principal investigator for Chilean observing time on the APEX telescope and, with C.V., observed the galaxy in CO and at 870 μm, reduced the relevant data in Table 1 and did relevant calculations for Table 2; D.A.H. determined the observational strategy, selected WLM for study, chose the observing coordinates, extracted the H I spectra from the LITTLE THINGS data and prepared Fig. 1. E.B. was principal investigator on the APEX proposal using European time through ESO and coordinated the work on data uncertainties and background noise. A.S. made the WLM H I data cube from Jansky Very Large Array observations. All authors discussed the results and commented on the manuscript.

Author Information Reprints and permissions information is available at www.nature.com/reprints. The authors declare no competing financial interests. Readers are welcome to comment on the online version of the paper. Correspondence and requests for materials should be addressed to and requests for materials should be addressed to B.G.E. (bge@us.ibm.com).